American Mineralogist, Volume 94, pages 704–709, 2009

High-pressure behavior of åkermanite and gehlenite and phase stability of the normal structure in melilites

Marco Merlini,[1,*] Mauro Gemmi,[2] Michael Hanfland,[1] and Wilson Crichton[1]

[1]ESRF, European Synchrotron Radiation Facility, 6 Rue Jules Horowitz, BP220, 38043 Grenoble CEDEX, France
[2]Dipartimento di Scienze della Terra "Ardito Desio," Università degli Studi di Milano, via Botticelli, 23, I-20133 Milano, Italy

Abstract

Åkermanite ($Ca_2MgSi_2O_7$) and gehlenite ($Ca_2Al_2SiO_7$) have been studied at high pressure by synchrotron radiation powder and single-crystal diffraction up to 30 GPa. At about 2 GPa, the incommensurately modulated structure (IC) transforms to a normal structure (N). The bulk modulus for the N structure, fitted with a Birch Murnhagan EoS on powder data, is 93.5(5) GPa. The compressibility is anisotropic, and it is greater along the *c* axis, in the direction perpendicular to the tetrahedral layers of the structure. Above 15 GPa, a phase transition is observed, marked by a discontinuity in the elastic behavior and a small change in intensity and in the full-width at half maximum (FWHM) of the powder diffraction peaks. The diffraction patterns are indexed with respect to tetragonal cell of the N-melilite structure up to 30 GPa. A hysteresis in the elastic behavior is observed during decompression. In contrast, single-crystal data show a new monoclinic phase appearing above 15 GPa. The unit-cell parameters are a = 8.82(1) Å, b = 7.34(1) Å, c = 9.13(1) Å, β = 115.1(2)°. This unit cell is similar to that of $Ca_2ZnGe_{1.25}Si_{0.75}O_7$ reported in the literature. A refinement using the corresponding model in space group $P2_1/n$ fits the single-crystal data with a reasonable R_{Bragg} = 15%, considering that the crystal is twinned and the mosaicity is large. Gehlenite has a higher bulk modulus, 106.1(4) GPa, than does åkermanite. The compressibility is anisotropic, and the behavior is similar to that of åkermanite, but the presence of Al in tetrahedral sites decreases the compressibility parallel to the (001) plane. The structure of gehlenite is stable up to 25 GPa, when a phase transition occurs.

Keywords: Melilite, high pressure, single crystal, compressibility, phase transition

Introduction

The melilites constitute an interesting mineral group. They are among the most primitive materials in the Ca-Al-rich inclusions in chondritic meteorites. They are also present in contact metamorphic and in magmatic rocks. Melilites are also present in industrial slags and cements. Åkermanite, $Ca_2MgSi_2O_7$, has been studied extensively (e.g., Hagiya et al. 1993; McConnell et al. 2000; Kusaka et al. 2001 and references therein), because it exhibits unique features, in particular the presence of a 2D incommensurately modulated structure (IC) at ambient conditions. At ambient pressure and 80 °C, a phase transition from the IC structure to the normal (N) one is observed (Hemingway et al. 1986; Rothlisberger et al. 1990). At ambient temperature, the increase of pressure promotes the transition to the N phase at about 1.7 GPa (Yang et al. 1997; McConnell et al. 2000). The stability of the IC structure is hence restricted to low-T and low-P conditions. The gehlenite substitution in åkermanite lowers the temperature of the IC/N transition (Merlini et al. 2005), and for gehlenite content higher than 20%, the N structure is stable at ambient conditions. In this paper, we report the results of high-pressure X-ray diffraction studies to investigate the elastic behavior of melilites and to define the high-pressure stability of the N-åkermanite structure. We have studied synthetic åkermanite and gehlenite samples. Melilite is tetragonal, and the structure is composed of layers of (Si,Al) and (Mg,Al) tetrahedra connected by Ca in eightfold coordination between the layers. The IC structure can be described as the result of a rotation of the (Si,Al) tetrahedra with respect to the average position (with a non-commensurate periodicity), and consequently as a slight distortion of the (Mg,Al) tetrahedra. In the IC structure, the Ca sites are non-equivalent and Ca sites with 6-, 7-, and 8-coordination are present. The relative number of 6-, 7-, and 8-coordinated sites and their distribution in the structure is a function of P, T, and composition.

Experimental methods

Synthesis of åkermanite and gehlenite is described elsewhere (Merlini et al. 2005). The high-pressure diffraction experiments were performed at the beamline ID09A, at ESRF (Grenoble, France). We used a membrane-type diamond-anvil cell (DAC), with He as pressure-transmitting medium. The pressure was measured by the ruby fluorescence method (Forman et al. 1972). X-ray wavelength was 0.413 Å. The detector used was a Mar345 imaging plate. Powder data were collected during DAC ω-oscillations of about 20°. Single-crystal data collections were performed with 60° ω scans with 2° step size. The experiments were performed up to 30 GPa, and some points were been collected during decompression. The powder IP data were integrated with the Fit2D software (Hammersley et al. 1996), masking all the diffraction peaks of diamond and solid He. The data have been analyzed with the Rietveld method using the GSAS software (Larson and Von Dreele 1988). Background was previously subtracted using the software DatLab (K. Syassen, pers. comm.). Single-crystal data have been reduced with the CrysAlis software package (Oxford diffraction 2006) and analyzed with the Jana2006 software package (Petricek et al. 2006). The pressure-volume data have been fit to a third-order Birch-Murnagham

* E-mail: merlini@esrf.fr

equation of state (Birch 1952; Angel 2000). Following Angel (2000), estimates of the linear moduli along the crystallographic axes have been obtained by a fit of the Birch-Murnagham EoS on the cubes of the unit-cell parameters.

RESULTS

In Figures 1 and 2, the lattice parameters and volume of åkermanite and gehlenite are plotted as functions of pressure. In the low-pressure data of åkermanite (Fig. 1), the behavior of the *c* lattice parameter indicates that the IC-N phase transition occurs at about 1.7 GPa, in agreement with Yang et al. (1997) and McConnell et al. (2000). The bulk modulus of the IC phase is 99(8) GPa. Analysis of the IC modulation peaks with single-crystal data indicates no change of the *q* modulation vector length as a function of pressure. In the pressure range 2–15 GPa no discontinuity in the volume and axial compressibility of the N structure is detected. The data, fit with a Birch-Murnagham EoS (1), give a volumetric bulk modulus of 93.5(5) GPa (K' = 4) or K_0 = 101(2) GPa, K' = 2.8(3), V_0 = 306.4(1), and a linear modulus of 99.0(7) GPa along *a* and 84.0(3) GPa along *c*. The N structure is therefore more compressible perpendicular to the tetrahedral layers than within the layers. Above 15 GPa, a phase transition is evident, marked by a discontinuity in the lattice parameters and volume behavior. The HP phase powder diffraction patterns do not show any major changes, and they can be indexed with the same tetragonal cell (Fig. 3). However,

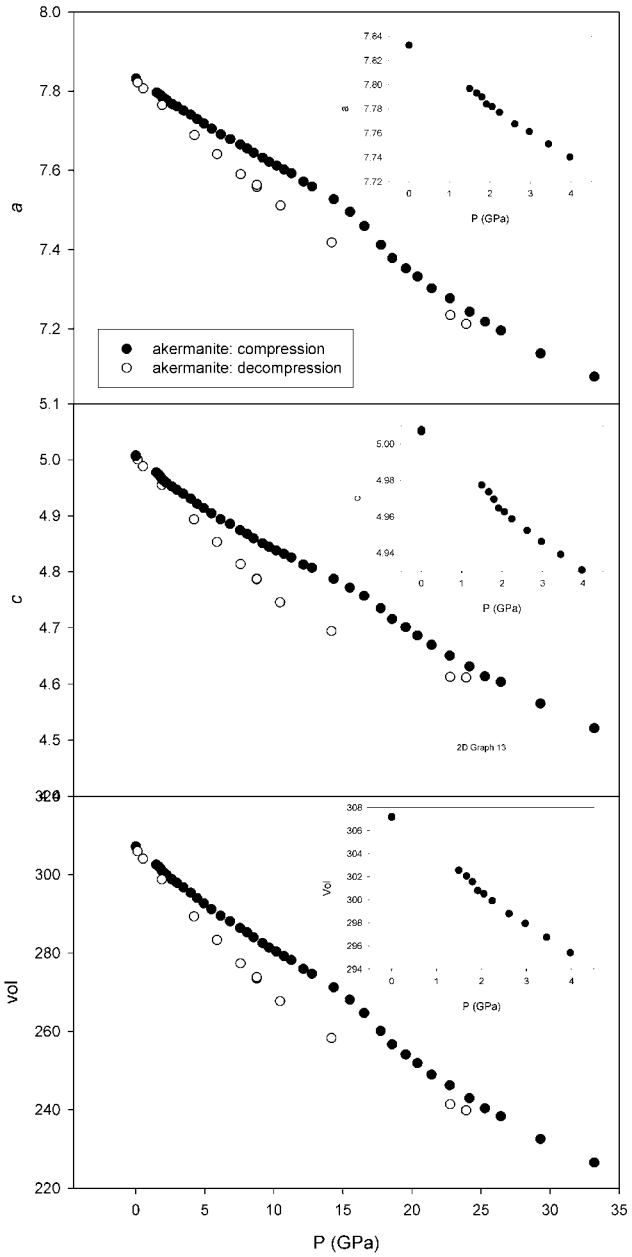

FIGURE 1. Unit-cell parameters *a*, *c*, and volume data for åkermanite during compression (filled circles) and decompression (empty circles). The errors are comparable with the symbol size. In the small boxes, the low-pressure data are zoomed.

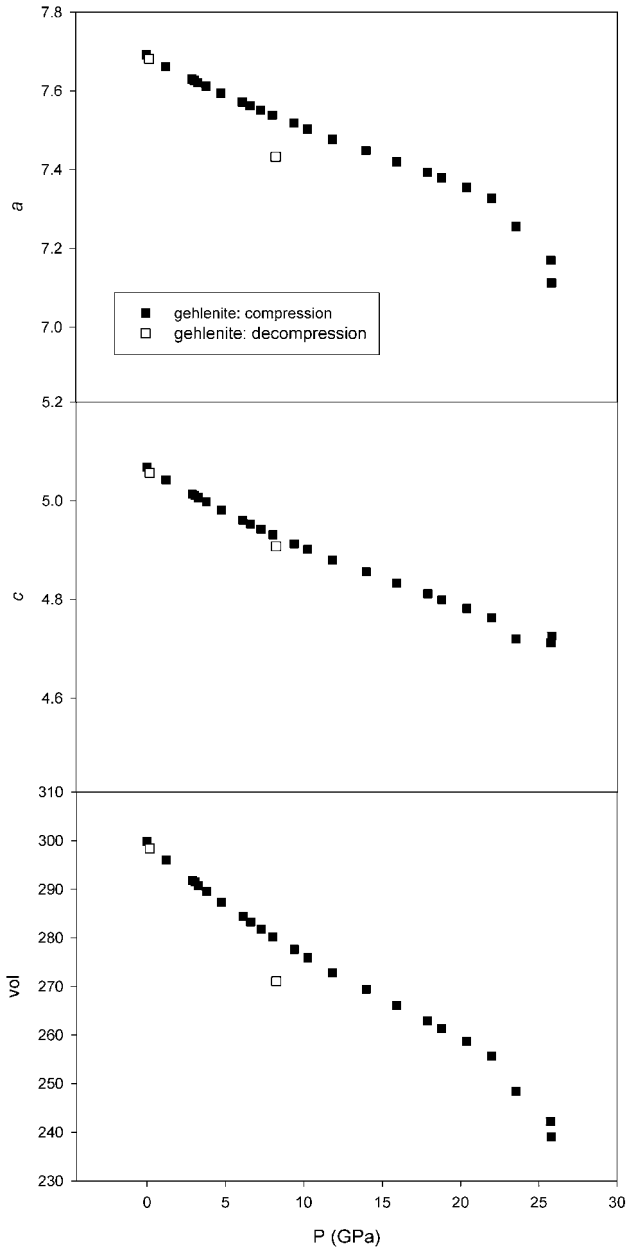

FIGURE 2. Unit-cell parameters *a*, *c*, and volume data for gehlenite during compression (filled squares) and decompression (empty squares). The errors are comparable with the symbol size.

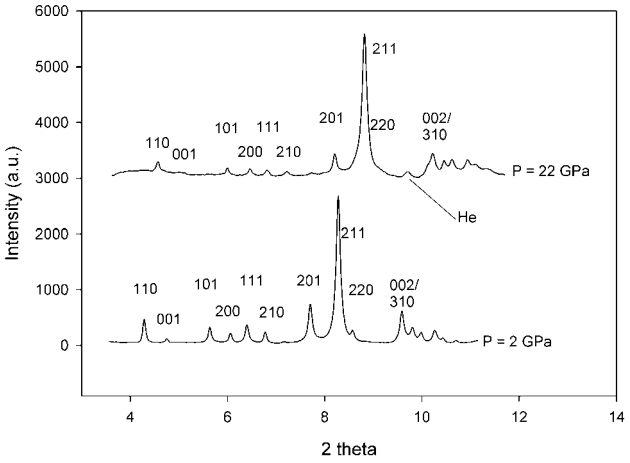

FIGURE 3. Powder patterns of N-åkermanite (P = 2 GPa) and HP phase (P = 22 GPa).

the compressibility of the HP phase increases, as suggested by the increased slope of the lattice parameter data in Figure 1. A fit of the HP data in the pressure range 18–35 GPa gives a bulk modulus of 30(7) GPa.

Single-crystal data have been collected to provide insight into the structural features of the high-pressure phase. Crystal-structure refinements of data collected up to 15 GPa (Table 1) reveal that in åkermanite, the Mg tetrahedron is softer than the Si tetrahedron, a trend that is also in agreement with the thermal behavior of melilites (Yang et al. 1997; Merlini et al. 2008). The Mg polyhedra become more regular with increasing pressure, while the Si tetrahedra become more distorted, Figure 4. The pressure was increased very slowly above 15 GPa. At 15.6 GPa, new diffraction peaks appeared. Surprisingly, it was no longer possible to index the diffraction peaks with the tetragonal cell, as in the powder experiment. The new HP-phase is monoclinic, with a = 8.82(1) Å, b = 7.34(1) Å, c = 9.13(1) Å, β = 115.1(2)°. This monoclinic cell is geometrically related to the original tetragonal one in the following way: $\mathbf{a}_{mon} = \mathbf{a}_{tet} - \mathbf{c}_{tet}$; $\mathbf{b}_{mon} = \mathbf{b}_{tet}$; $\mathbf{c}_{mon} = 2\mathbf{c}_{tet}$. After the phase transition, it was found that the crystal is twinned by a rotation of 90° around [101]. The cell is similar to the low-$Ca_2ZnGe_{1.25}Si_{0.75}O_7$ unit cell identified by Armbruster et al. (1990). Systematic extinctions are compatible with space group $P2_1/n$ (Fig. 5) used by Armbruster et al. (1990) and Redhammer et al. (2006), respectively, in the $Ca_2ZnGe_{1.25}Si_{0.75}O_7$ and $Ca_2Zn_{0.97}Co_{0.03}Ge_2O_7$ structure refinements. About 80% of the diffraction spots are indexed by the two main twin domains identified. Other peaks belong to other monoclinic crystals slightly misaligned with respect to the main twins, because the

TABLE 1. Refined atomic coordinates by single-crystal diffraction of N-åkermanite structure and of the monoclinic high-pressure phase

	x	*y*	*z*
		***P* = 5 GPa**	
Mg1	0	0	0
Ca1	0.3343(3)	0.1657(3)	0.5065(16)
Si1	0.1416(4)	0.3584(4)	0.937(2)
O1	0	0.5	–0.195(6)
O2	0.1438(9)	0.3562(9)	0.260(5)
O3	0.0803(9)	0.1843(8)	0.782(3)
		***P* = 15 GPa**	
Mg1	0	0	0
Ca1	0.3371(2)	0.1629(2)	0.5042(12)
Si1	0.1430(4)	0.3570(4)	0.9392(15)
O1	0	0.5	–0.198(5)
O2	0.1421(8)	0.3579(8)	0.268(3)
O3	0.0807(8)	0.1841(6)	0.774(3)
		***P* = 15.7 GPa**	
Mg1	0.8107(11)	0.0997(7)	0.0926(11)
Si1	0.8648(7)	0.4512(5)	0.2150(8)
Si2	0.9575(6)	0.7554(3)	0.0731(5)
Ca1	0.4593(5)	0.2794(3)	0.0294(5)
Ca2	0.3028(4)	0.5638(3)	0.2121(4)
O1	0.9975(12)	0.5618(7)	0.1593(12)
O2	0.8801(16)	0.5221(11)	0.3791(16)
O3	0.698(3)	0.4728(19)	0.041(3)
O4	1.0049(19)	0.8800(12)	0.2257(19)
O5	1.1263(9)	0.8208(6)	0.0662(9)
O6	0.9530(12)	0.2625(6)	0.2856(11)
O7	0.783(2)	0.7583(10)	–0.097(2)

Notes: The refinement of the N-åkermanite structure has been performed in space group $P\bar{4}2_1n$. The lattice parameters at 5 and 15 GPa are, respectively, a = 7.740(6) and 7.570(6); c = 4.932(6) and 4.781(6). The number of independent diffractions used are 150 and 147 (1200 total). R_{int} = 3.8 and 4.2%. R1 = 6.7 and 6.9%. The monoclinic cell at 15.7 GPa is a = 8.82(1) Å, b = 7.34(1) Å, c = 9.13(1) Å, β = 115.1(2)°, space group $P2_1/n$. 1000 total diffractions have been used (650 independent). R_{int} = 8.2%. R1 = 15%.

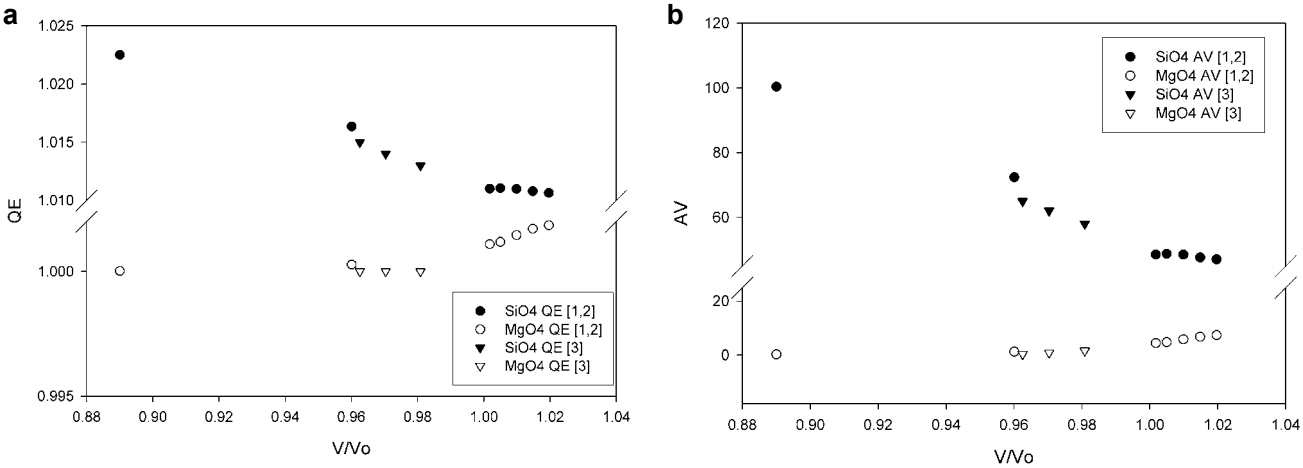

FIGURE 4. Quadratic elongation, QE, (**a**) and angle variance, AV, (**b**) of SiO_4 and MgO_4 tetrahedra, plotted against normalized volume. In the figure, HP data [1] = this work, high-pressure crystal structure refinements at 5 and 15 GPa, HT data, [2] = Merlini et al. (2008) and HP data, [3] = Yang et al. (1997) are reported. QE and AV, two parameters to quantify the distortion of coordination polyhedra, are calculated according to Hazen and Finger (1982).

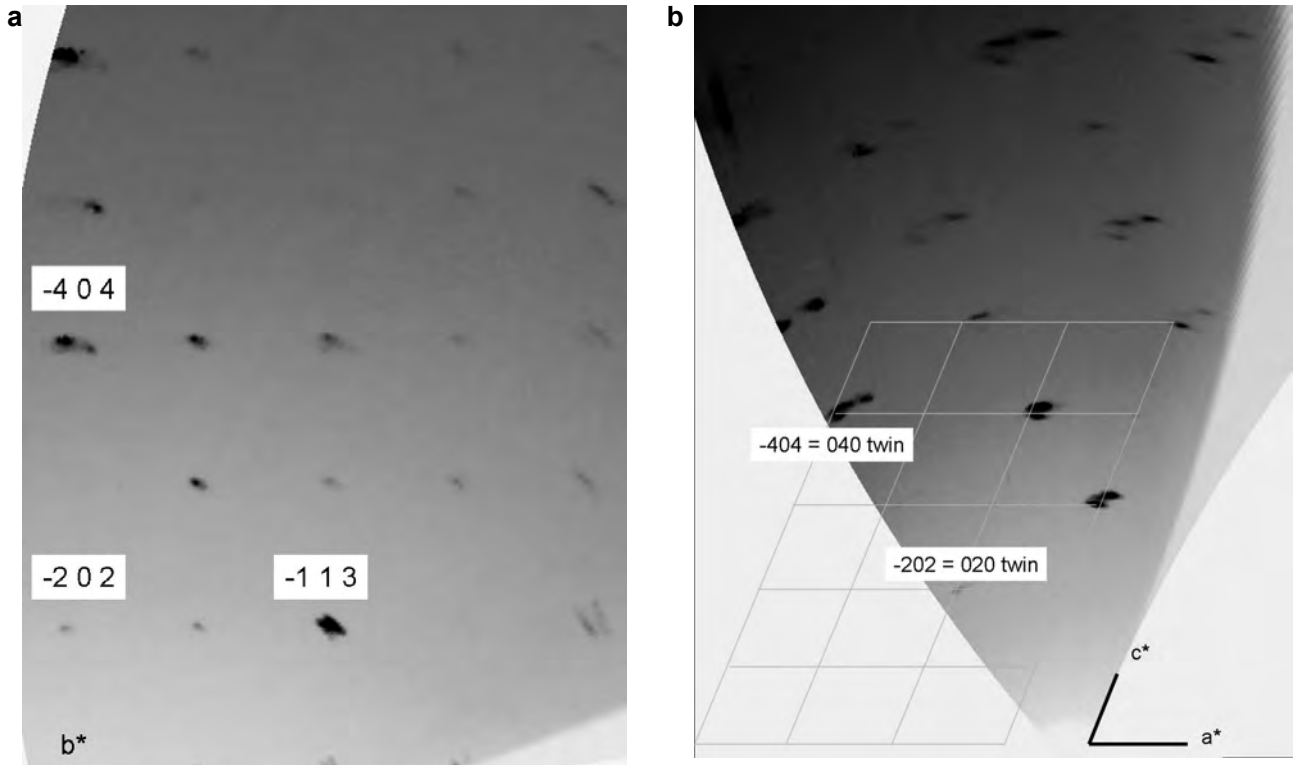

FIGURE 5. Reciprocal space reconstruction of the a^*b^* plane (**a**) and a^*c^* plane (**b**). In **a**, the indexation is trivial, and the indices reported refer to the diffraction almost coinciding with the second twin. The twinning explains why $0k0$ $k = 2n$ are not extinct in the figure. In **b**, the reflection conditions $h + k = 2n$ are clearly visible.

crystal probably broke after the phase transition.

Refinement of the crystal structure, using the structural model of Ambruster et al. (1990) on twinned data gives an R_{Bragg} value of 15%. The structure is shown in Figure 6. The refinement has been first carried out with constraints on Si-O and Mg-O distances, and finalized without any constraints. The refined atomic coordinates are reported in Table 1 and interatomic distances are in the supplementary tables[1]. It is difficult to assess the accuracy of the results, since it is difficult to detect and separate possible systematic errors that affect the refinement, mainly due to increased crystal mosaicity related to the presence of slightly misaligned crystal domains. However, it is notable that the Si-O distances are within the expected range of values for high-pressure SiO_4 tetrahedra. If the refined model is accurate, a comparison with the Armbruster et al. (1990) monoclinic structure reveals that the Mg-O tetrahedra are more distorted and two additional Mg-O bonds of 2.8 Å are present. A similar feature is present in [6]-coordinated Ca site. In the low-$Ca_2ZnGe_{1.25}Si_{0.75}O_7$ structure, there are only six Ca-O distances shorter than 3 Å (average Ca-O distance is 2.4 Å). In the high-pressure phase, an additional Ca-O distance of about 2.6 Å increases the coordination number of the site.

High-pressure measurements have been performed also on gehlenite with a powder sample, to investigate the influence of Al substitution on the high-pressure behavior of melilites. The bulk modulus for gehlenite is 106.1(4) GPa with K' fixed at 4, and $K_0 = 104(1)$, $K' = 4.3(2)$, $V_0 = 299.6(1)$ with a third-order fit. The linear moduli along a and c are 120.8(5) and 84.1(3) GPa, respectively. The high-pressure data of gehlenite also indicate a discontinuity in the elastic behavior at high pressure, as seen for åkermanite, but at higher pressure, above 25 GPa a change in elastic behavior is detected. The effect of Al substitution in åkermanite then seems to increase the pressure of the transition. The powder pattern of gehlenite above 25 GPa is still indexable with a tetragonal cell.

DISCUSSION

A comparison between the elastic behavior of åkermanite and gehlenite (N-structure) reveals several interesting features. The bulk modulus increases from åkermanite to gehlenite (especially evident comparing the data obtained with a fit with the

[1] Deposit item AM-09-026, Supplementary Tables. Deposit items are available two ways: For a paper copy contact the Business Office of the Mineralogical Society of America (see inside front cover of recent issue) for price information. For an electronic copy visit the MSA web site at http://www.minsocam.org, go to the American Mineralogist Contents, find the table of contents for the specific volume/issue wanted, and then click on the deposit link there.

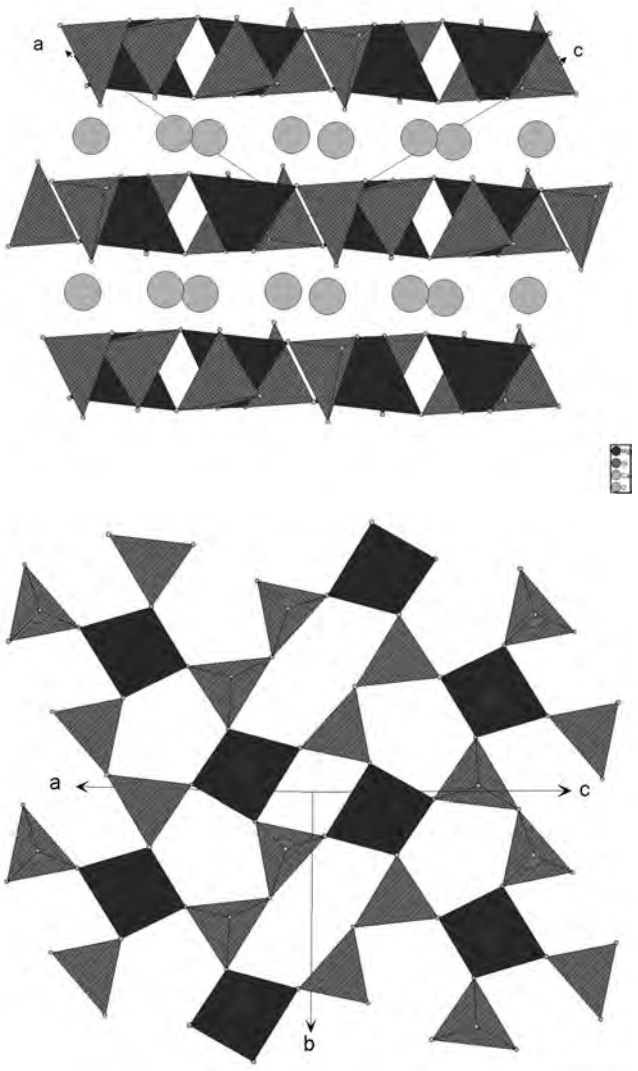

FIGURE 6. Crystal structure of the monoclinic HP phase. It consists of layers of MgO_4 and SiO_4 tetrahedra connected by Ca cations. The topology of the tetrahedral layers (Armbruster et al. 1990) presents 4-, 5-, and 6-membered rings, while the melilite structure presents only 5-member rings. In the figure, the dark gray tetrahedra are the MgO_4 tetrahedra; the light gray tetrahedra are the SiO_4 tetrahedra.

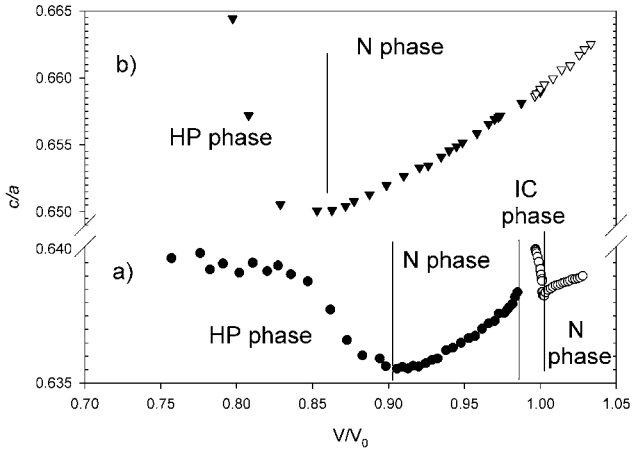

FIGURE 7. "Inverse relationship" (Hazen and Finger 1982) for åkermanite (**a**) and gehlenite (**b**). Plot of the *c*/*a* ratio vs. normalized volume (298 K, 1 bar). Circles = åkermanite. Triangles = gehlenite. Empty symbols = this work. Filled symbols = high-/low-temperature data (Merlini et al. 2005). The pressure of transition is 15 GPa (åkermanite) and 25 GPa (gehlenite). The features of åkermanite in the region close to $V/V_0 = 1$ refer to the IC-N phase transition.

constraint of $K' = 4$). The density at ambient conditions is also greater in gehlenite (3.04 g/cm^3) than in åkermanite (2.95 g/cm^3). The results are in agreement with their HT behavior (Merlini et al. 2005). In the åkermanite-gehlenite series, the elasticity along the *c* direction (perpendicular to the tetrahedral layers) is similar and independent of composition within our resolution, with a linear modulus value close to 84 GPa. The main difference is the elasticity along the *a* direction, that is, within the tetrahedral layers. The compressibility is, in fact, greater in åkermanite, where the tetrahedral T1 site is fully occupied by Mg. An analysis of the axial ratio (*c*/*a*) behavior as a function of *P* (Fig. 7) can give some insight in the high-pressure behavior and phase transition of melilite. Figure 7 shows that the evolution of the axial ratio with pressure is almost linear up to a critical pressure, where a discontinuity is observed. To better evaluate the change of the =*c*/*a* ratio, in Figure 7 the data are plotted as a function of the normalized volume. Also high- and low-temperature data measured on the same samples are plotted in the same figure, following the "inverse relationship" concept (Hazen and Finger 1982). From the figures, it is evident that the high-temperature data correlate very well with high-pressure data up to a critical pressure. In åkermanite, in the range 0.98–1.05 V/V_0, the data do not correlate because of the IC/N phase transition (Merlini et al. 2005). The deviation from the linear trend at high pressure indicates a rearrangement of the structure. The increase of the *c*/*a* ratio with respect to the extrapolated value of the N-melilite structure, as well as the hysteresis in the behavior of the lattice parameters during decompression (which correlates to the ambient pressure IC phase without any significant discontinuity), suggest a close relationship between the IC phase observed at ambient pressure and the HP phase observed with the powder data. The origin of the IC-structure in åkermanite is ascribed to a structural misfit of the tetrahedral layer with the Ca-layer (Rotlisberger et al. 1990; Bindi et al. 2001). The structural strain is then accommodated at low *T* by a modulation of the structure. At high pressure, it appears that the stability of N-melilite structure is also limited. Powder data exhibit a minor re-arrangement of the structure. The symmetry remains tetragonal, but unfortunately, we are not able to identify whether the HP structure is modulated (but even ambient *P* powder data do not show any modulation, essentially because the Compton scattering of diamonds hides any weak diffraction signal for low scattering material). In contrast, single-crystal samples transform to a monoclinic phase, which has already been observed to appear at low *T*, below the stability field of the N-melilite structure. The monoclinic structure has been observed also in other single-crystal experiments on åkermanite. Unfortunately the crystal completely broke down above 15 GPa, probably because pressure increase was too fast. However, the powder-like pattern (Fig. 8) is indexable with the same monoclinic cell. It is notable that the monoclinic phase is

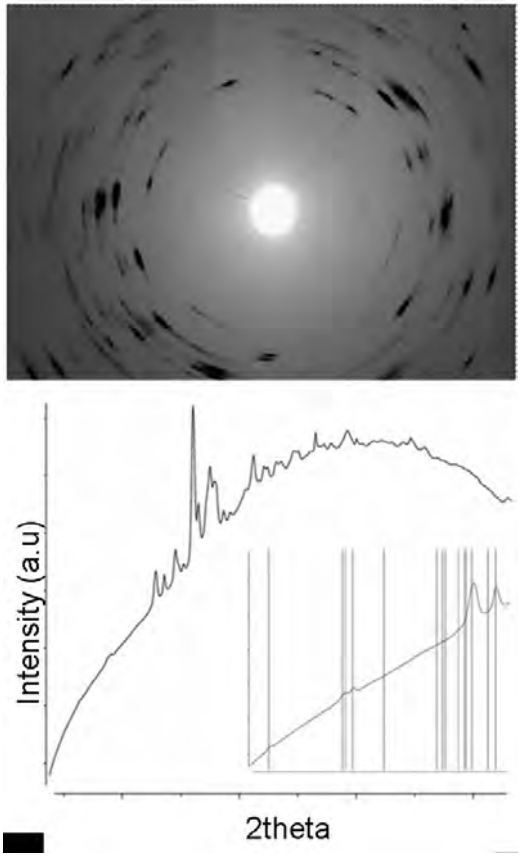

FIGURE 8. Powder-like pattern of a single crystal of åkermanite after the N-HP phase transition at about 15 GPa. The integrated powder pattern is different from the N-åkermanite, especially at low angle. In the figure, a zoomed region of the low angle diffraction pattern is reported, together with the marker of the diffraction peaks position of the monoclinic $P2_1/n$ cell.

not related to the N-melilite phase by a displacive transition, as is the IC-phase, since the topology of the tetrahedral layer is different (Armbruster et al. 1990). Fine grinding of the sample could have produced some annealing in the crystals, and the system could evolve toward a displacive transition. On the other hand, the presence of defects, which are not uncommon in the melilite samples analyzed (Gemmi et al. 2007), as well as minor shear strain (even though He has been used as pressure transmitting medium) could trigger the transformation into a reconstructive phase transition. Moreover, it could also be considered that surface energy could play a role during a phase transition in a single crystal compared to fine powder samples.

ACKNOWLEDGMENTS

The high-pressure experiments were performed at ESRF, at the beamline ID09A, during the beam time allocated for experiment HS-3398 and in-house research. Karl Syassen is acknowledged for helpful discussions and provision of DatLab software. Critical comments by R. Downs, by an anonymous reviewer and by the associate editor have been very useful to improve the quality of the manuscript.

REFERENCES CITED

Angel, R.J. (2000) High-pressure, high-temperature crystal chemistry. In R.M. Hazen and R.T. Downs, Eds., High-Temperature and High-Pressure Crystal Chemistry, 41, p. 35–59. Reviews in Mineralogy and Geochemistry, Mineralogical of Society America, Chantilly, Virginia.

Armbruster, T., Rothlisberger, F., and Seifert, F. (1990) Layer topology, stacking variation and site distortion in melilite-related compounds in the system CaO-ZnO-GeO_2-SiO_2. American Mineralogist, 75, 847–858.

Bindi, L., Bonazzi, P., Dusek, M., Petricek, V., and Chapuis, G. (2001) Five-dimensional structure refinement of natural melilite, $(Ca_{1.89}Sr_{0.01}Na_{0.08}K_{0.02})(Mg_{0.92}Al_{0.08})(Si_{1.98}Al_{0.02})O_7$. Acta Crystallographica, B57, 739–746.

Birch, F. (1952) Elasticity and constitution of the Earth's interior. Journal of Geophysical Research, 57, 227–286

Forman, R.A., Piermarini, G.J., Barnett, J.D., and Block, S. (1972) Pressure measurement made by utilization of ruby sharp-line luminescence. Science, 176, 284–286.

Gemmi, M., Merlini, M., Cruciani, G., and Artioli, G. (2007) Non-ideality and defectivity of the åkermanite-gehlenite solid solution: An X-ray diffraction and TEM study. American Mineralogist, 92, 1685–1694.

Hagiya, K., Ohmasa, M., and Iishi, K. (1993) The modulated structure of synthetic Co-åkermanite, $Ca_2CoSi_2O_7$. Acta Crystallographica, B49, 172–179.

Hammersley, A.P., Svensson, S.O., Hanfland, M., Fitch, A.N., and Häusermann, D. (1996) Two-dimensional detector software: From real detector to idealized image or two-theta scan. High Pressure Research 14, 235–245.

Hazen, R.M. and Finger, L.W. (1982) Comparative Crystal Chemistry. Wiley, New York.

Hemingway, B.S., Evans Jr., H.T., Nord Jr., G.L., Haselton Jr., H.T., Robie, R.A., and McGee, J.J. (1986) Åkermanite: Phase transitions in heat capacity and thermal expansion, and revised thermodynamic data. Canadian Mineralogist, 24, 425–434.

Kusaka, K., Hagiya, K., Ohmasa, M., Okano, Y., Mukai, M., Iishi, K., and Haga, N. (2001) Determination of structures of $Ca_2CoSi_2O_7$, $Ca_2MgSi_2O_7$, and $Ca_2(Mg_{0.55}Fe_{0.45})Si_2O_7$ in incommensurate and normal phases and observation of diffuse streaks at high temperature. Physics and Chemistry of Minerals, 28, 150–166.

Larson, A.C. and Von Dreele, R.B. (1988) General Structure Analysis System (GSAS). Report LAUR 86-748. Los Alamos National Laboratory, New Mexico.

McConnell, J.D.C., McCammon, C.A., Angel, R.J., and Seifert, F. (2000) The nature of the incommensurate structure in åkermanite, $Ca_2MgSi_2O_7$, and the character of its transformation from the normal structure. Zeitschrift für Kristallographie, 215, 669–677.

Merlini, M., Gemmi, M., and Artioli, G. (2005) Thermal expansion and phase transitions in åkermanite and gehlenite. Physics and Chemistry of Minerals, 32, 189–196.

Merlini, M., Gemmi, M., Cruciani, G., and Artioli, G. (2008) High-temperature behavior of melilite: In situ X-ray diffraction study of gehlenite-åkermanite-Na melilite solid solution. Physics and Chemistry of Minerals, 35, 147–155.

Oxford Diffraction (2006) Crysalis RED, version 1.171.31.8. Oxford Diffraction Ltd., Abingdon, Oxfordshire.

Petricek, V., Dusek, M., and Palatinus, L. (2006) Jana2006. The crystallographic computing system. Institute of Physics, Praha, Czech Republic.

Redhammer, G.J. and Roth, G. (2006) Commensurate monoclinic form of $Ca_2Zn_{0.97}Co_{0.03}Ge_2O_7$. Acta Crystallographica, C62, i61–i63.

Rothlisberger, F., Seifert, F., and Czank, M. (1990) Chemical control of the commensurate-incommensurate phase transition in synthetic melilites. European Journal of Mineralogy, 2, 585–594.

Yang, H., Hazen, R.M., Downs, R.T., and Finger, L.W. (1997) Structural change associated with the incommensurate-normal phase transition in åkermanite, $Ca_2MgSi_2O_7$ at high pressure. Physics and Chemistry of Minerals, 24, 510–519.

MANUSCRIPT RECEIVED AUGUST 8, 2008
MANUSCRIPT ACCEPTED FEBRUARY 2, 2009
MANUSCRIPT HANDLED BY PRZEMYSLAW DERA